Received: 16 August 2017 | Revised: 10 December 2017 | Accepted: 18 January 2018

DOI: 10.1002/bio.3468

RESEARCH ARTICLE

WILEY LUMINESCENCE
The Journal of Biological and Chemical Luminescence

Highly selective and sensitive coumarin–triazole-based fluorometric 'turn-off' sensor for detection of Pb^{2+} ions

Shaily[1,2] | Ajay Kumar[2] | Iram Parveen[1] | Naseem Ahmed[1]

[1] Department of Chemistry, Indian Institute of Technology, Roorkee, India

[2] Department of Chemistry, D.B.S. (P.G.) College Dehradun, India

Correspondence
Shaily and Naseem Ahmed, Department of Chemistry, Indian Institute of Technology, Roorkee 247667, India.
Email: shailydbs@gmail.com; nasemfcy@iitr.ac.in

Funding information
Ministry of Human Resource and Development (MHRD), New Delhi, India, Grant/Award Number: MHR01-23-200-428

Abstract

Exposure to even very low concentrations of Pb^{2+} is known to cause cardiovascular, neurological, developmental, and reproductive disorders, and affects children in particular more severely. Consequently, much effort has been dedicated to the development of colorimetric and fluorescent sensors that can selectively detect Pb^{2+} ions. Here, we describe the development of a triazole-based fluorescent sensor **L5** for Pb^{2+} ion detection. The fluorescence intensity of chemosensor **L5** was selectively quenched by Pb^{2+} ions and a clear color change from colorless to yellow could be observed by the naked eye. Chemosensor **L5** exhibited high sensitivity and selectivity towards Pb^{2+} ions in phosphate-buffered solution [20 mM, 1:9 DMSO/H_2O (v/v), pH 8.0] with a 1:1 binding stoichiometry, a detection limit of 1.9 nM and a 6.76×10^6 M^{-1} binding constant. Additionally, low-cost and easy-to-prepare test strips impregnated with chemosensor **L5** were also produced for efficient of Pb^{2+} detection and proved the practical use of this test.

KEYWORDS

coumarin, fluorescence, Pb^{2+} ion, sensor, triazole

1 | INTRODUCTION

Heavy-metal pollution in the environment due to industrialization and urbanization is a serious issue worldwide especially in developing countries, and has attracted growing attention from researchers and scientists. Among the heavy-metal ions cadmium, lead and mercury, lead is the most abundant and toxic element. Around 300 million tonnes of mined lead are still circulating in aquatic systems (i.e. in ground water, surface water and aquifers) and soil, such that these polluted aquatic systems and soils have become a serious threat to the environment, and animal and human health.[1,2] Toxic lead enters the environment through its use in waste plastic, dyes, heavy fuel oils, batteries, gasoline and blast furnaces, etc. In addition lead, due to its non-degradable nature, is an environmental pollutant and difficult to detoxify by chemical or biological means, thereby resulting in contaminated portable water and food.[3] Exposure to lead ions may cause serious health problems in humans and especially in children such as muscle paralysis, irritability, neurological, cardiovascular, and developmental disorders, hypertension, mental retardation and slowed motor responses. Lead even affects human soft tissues and organs causing cancer and acts synergistically with other carcinogens.[4,5] Low concentrations of lead in the human body act as a powerful neurotoxin that can trigger behavioural problems, interfere with brain development and slow nerve conduction speeds.[6–8] The most common molecular targets of lead include zinc- and calcium-binding proteins that control gene expression and cell signalling, respectively, and lead to protein disfunction.[9] Therefore, due to their hazardous nature, heavy metals, especially lead, cadmium and mercury, are banned by the European Union's Restriction of the Use of Certain Hazardous Substances (RoHS) in Electrical and Electronic Equipment Directive.[10] Moreover, permissible concentration limits of lead ions in drinking water have been rigorously defined by the United States Environmental Protection Agency (USEPA) and the World Health Organization (WHO) as 16 ppb (16 μg L^{-1}) and 10 ppb (48 nM) respectively.[11,12] Likewise, an action level of 2.5 μM for lead in products anticipated for use by infants and children has been set by the United States Food and Drug Administration.[13] Therefore, determination and monitoring of lead levels are very important to ensure that heavy-metal lead concentrations remain below the defined toxic level. Several sophisticated analytical techniques such as inductively coupled plasma atomic emission spectroscopy (ICP-MS), anodic stripping voltammetry

Abbreviation used: AAS, atomic absorption spectroscopy; DFT, density functional theory; DMSO, dimethyl sulphoxide; ESI, electro spray-ionization; FT-IR, Fourier transform infra-red; HOMO, highest energy occupied molecular orbital; HRMS, high-resolution mass spectrum; LMCT, ligand-to-metal charge transfer; LUMO, lowest unoccupied molecular orbital; NMR, nuclear magnetic resonance; TLC, thin layer chromatography; UV, ultraviolet; WHO, World Health Organization.

and atomic absorption spectroscopy (AAS) are currently used for detection of Pb^{2+} in the environment.[14–16] However, most methods have several disadvantages such as cell impermeability, induced background expression and poor metal selectivity, plus these standard techniques can only measure total lead content. So, there is still a strong need to explore the use of rapid, easy to use, economical, highly sensitive and real-time monitoring techniques to detect trace levels of Pb^{2+}. In recent years, to meet this requirement, several research groups have developed highly sensitive fluorescent probes that selectively respond to lead ions.[17–25]

Coumarin and its derivatives are an important class of fluorescent compounds that have been used to construct various fluorescent chemosensors due to their excellent photophysical properties of small size and high quantum yield.[26–29] In an earlier publication we reported the synthesis of various functionalized coumarin-derived scaffolds as a cation–anion sensor[30–33], the current study focusses mainly on the design and development of efficient organic scaffolds that sensitively and selectively detect metal ions and anions in aqueous–organic media. Here we describe the development of a coumarin–triazole-based receptor 4-((1-(2-oxo-2*H*-chromen-4-yl)-1*H*-1,2,3-triazol-5-yl)methoxy)-2*H*-chromen-2-one **L5** for the identification of Pb^{2+} ions in a combined organic and aqueous medium.

2 | EXPERIMENTAL

Metal salts were purchased from HiMedia (Mumbai, India) and Loba Chemie (Mumbai, India); 4-hydroxycoumarin was purchased from Sigma Aldrich. All other general solvents and reagents were of analytical grade and used without further purification. For electronic and fluorescence spectral studies, spectroscopic grade DMSO and water were used. Thin layer chromatography was carried out on alumina-backed plates coated with Merck F254. ^{1}H and ^{13}C nuclear magnetic resonance (NMR) spectra of compounds were measured on a JEOL ECX-400-II spectrometer in $CDCl_3$ and DMSO-d_6, chemical shifts were reported on the δ scale in ppm (parts per million) with tetramethylsilane as an internal reference. Analysis of high-resolution mass spectra (HRMS) was performed on a Bruker microToF-Q-II electrospray-ionization (ESI) mass spectrometer. Fluorescence emission spectra were recorded between 400–600 nm (λ_{ex} = 390 nm) on a Fluoromax-4 spectrofluorometer using a 3-cm quartz cell. Ultraviolet (UV)–vis spectra were measured using a Shimadzu UV-2450 spectrophotometer. The pH of the solution was measured using a MRFS Toshniwal pH meter. Melting points of the compounds were measured using an Optimelt automated melting point apparatus. Fourier transform infra-red (FT-IR) spectra were recorded using an Alpha FT-IR spectrometer (Bruker) with the sample prepared in KBr pellets. Fluorescence quantum yields and lifetime spectra were measured using a fluorescence spectrometer FLS 980 (Edinburgh Instruments) and a Horiba Jobin Yvon Fluorocube lifetime system, respectively.

2.1 | Synthesis and characterization of 4-((1-(2-oxo-2*H*-chromen-4-yl)-1*H*-1,2,3-triazol-5-yl)methoxy)-2*H*-chromen-2-one (L5)

For the synthesis of title compound **L5**, first we synthesized precursors **1** and **3** from commercially available 4-hydroxycoumarin. Synthesis of **1** involved a single-step substitution reaction of 4-hydroxycoumarin with propargyl bromide. The two-step synthesis of **3** involved tosylation of 4-hydroxycoumarin followed by substitution of tosyl with azide. The detailed experimental procedure for the synthesis of the starting compounds **1**, **3** and the final compound **L5** are described below and in Scheme 1 (ESI, Figures S1-S5).

Step 1: Synthesis of 4-(prop-2-ynyloxy)-2*H*-chromen-2-one (1)[34]
A solution of propargyl bromide (237.92 mg, 2.0 mmol) in acetone was added to a stirred suspension of 4-hydroxycoumarin (324.24 mg, 2.0 mmol) and K_2CO_3 (276.41 mg, 2.0 mmol) in acetone, and the resulting reaction mixture was refluxed at 60°C for 12 h. After completion of the reaction, the solution was allowed to cool at room temperature and then poured into ice-cold water for precipitation. The precipitate was filtered and washed subsequently with water and acetone. The resulting precipitate was dried under vacuum and a pure product was obtained as a brown solid with a 95% (380 mg) yield. M.P. = 132°C; ^{1}H-NMR ($CDCl_3$, 400 MHz) δ = 2.68 (t, *J*= 2.20 Hz, 1H), 4.87 (d, *J* = 2.20 Hz, 2H), 5.83 (s, 1H), 7.26–7.30 (m, 2H), 7.62–7.64 (m, 1H), 7.82 (d, *J* = 7.32 Hz, 1H);^{13}C-NMR ($CDCl_3$, 100 MHz) δ = 65.8, 73.5, 77.0, 87.3, 118.6, 119.6, 126.5, 128.2, 129.3, 149.0, 158.3, 160.0; IR; ν_{max}(cm^{-1}) 3281, 3231, 3077, 2124, 1717, 1618, 1562, 1489, 1450, 1410, 1362, 1250, 1191, 1106, 987, 934, 841, 755, 650, 517, 476.

Step 2: Synthesis of 2-oxo-2*H*-chromen-4-yl 4-methylbenzenesulfonate (2)[35]

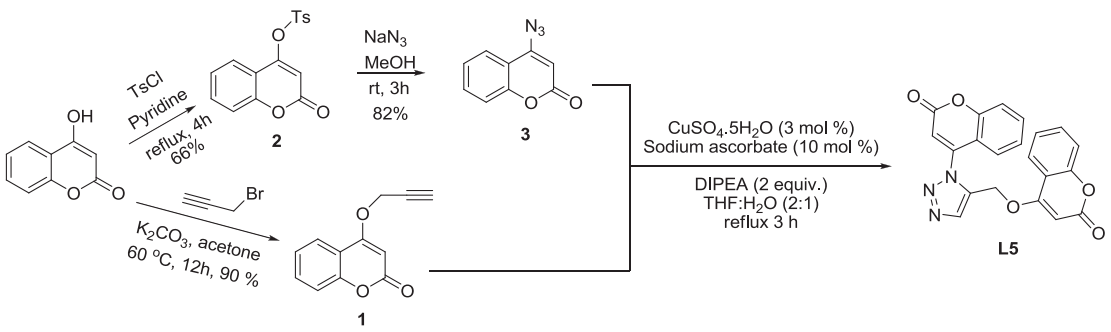

SCHEME 1 Synthesis route of chemosensor **L5**

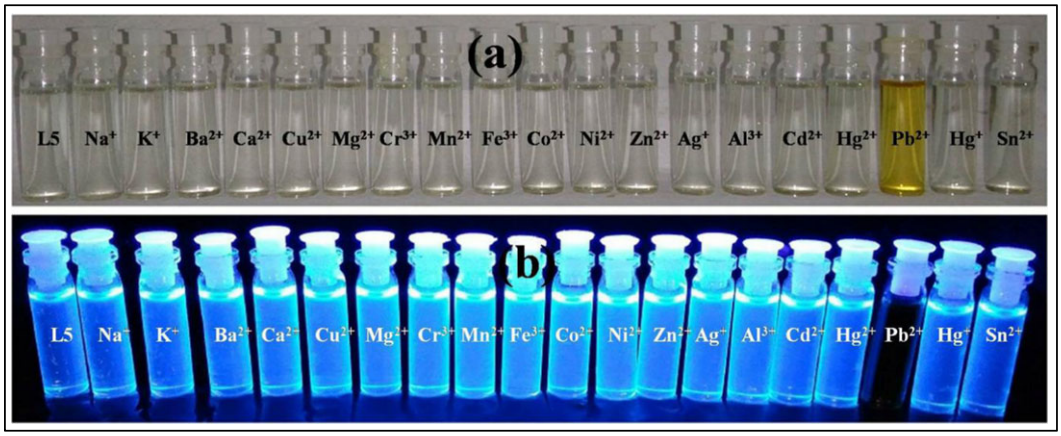

FIGURE 1 (a) Colorimetric (b) Fluorometric naked-eye detection of **L5** in absence and presence of various metal ions (20 equiv.) in phosphate-buffered solution [20 mM, 1:9 DMSO/H_2O (v/v), pH 8.0]

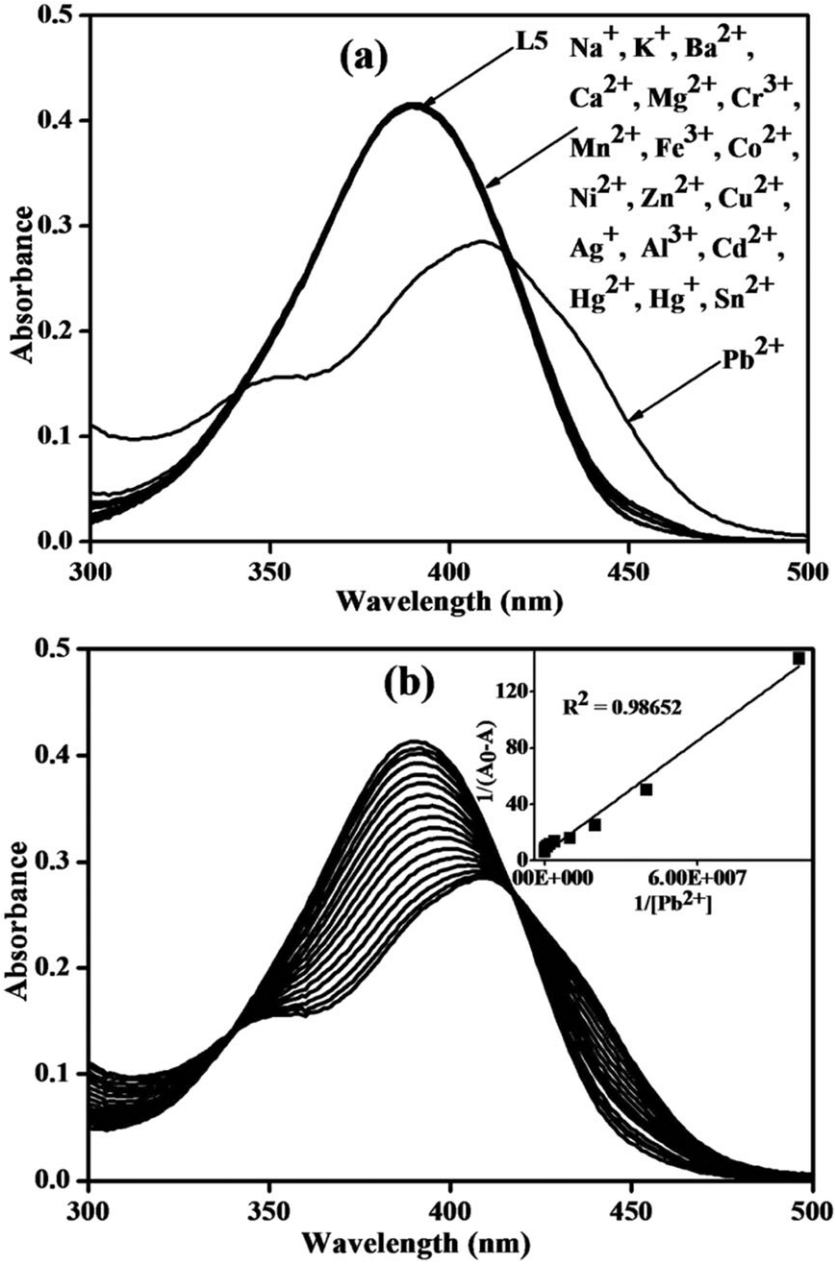

FIGURE 2 (a) UV–vis absorbance spectra of **L5** in the absence or presence of some metal ions. (b) UV–vis absorbance titration of **L5** with Pb^{2+}, concentrations ranging from 0 to 20 equiv.

Next, 6.0 mL of dry pyridine and 4-hydroxycoumarin (324.28 mg, 2.0 mmol) were added to a 25 mL round bottom flask, followed by the step-by-step addition of 1.0 equiv. of *p*-toluenesulfonyl chloride (380 mg, 2.0 mmol) at room temperature, the resulting reaction was refluxed and stirred continuously for 4 h. After completion of the reaction, the resulting mixture was poured into a beaker with ice-cold water to obtain a precipitate. The resulting precipitate was filtered, washed subsequently with cold water and dried under vacuum to get the pure product as a white solid with a 66% yield (417 mg) yield. M.P. = 112°C; ^{1}H-NMR (400 MHz, $CDCl_3$, ppm): δ 2.45 (s, 3H), 6.29 (s, 1H), 7.22–7.32 (m, 2H), 7.38 (d, *J* = 8.8 Hz, 2H), 7.51–7.59 (m, 1H), 7.63 (dd, *J* = 2.0, 8.4 Hz, 1H), 7.88 (d, *J* = 8.4 Hz, 2H); ^{13}C-NMR (100 MHz, $CDCl_3$, ppm): δ 21.7, 103.6, 115.0, 116.9, 123.2, 124.4, 128.4, 130.4, 131.7, 133.2, 146.8, 153.5, 157.8, 160.7; IR; ν_{max} (cm^{-1}) 3066, 2919, 2863, 1930, 1862, 1809, 1723, 1619, 1566, 1486, 1450, 1374, 1286, 1222, 1176, 1132, 1069, 932, 871, 820, 812, 750, 699, 585, 573, 538, 503.

Step 3: Synthesis of 4-azido-2*H*-chromen-2-one (3)[36]

To the solution of compound **2** (316.32 mg, 1.0 mmol) in methanol, 5 equiv. of sodium azide were added and resulting reaction mixture was continuously stirred for 3 h at room temperature. Then the reaction mixture was poured into a beaker of ice-cold water, and filtered to get the resulting precipitate, which was then washed with methanol and water. Finally the precipitate was dried under vacuum to get the pure product as a light brown powder in 82% (153 mg) yield. M.P. = 159°C; ^{1}H-NMR (400 MHz, $CDCl_3$, ppm): δ 6.13 (s, 1H), 7.27–7.32 (m, 1H), 7.32–7.39 (m, 1H), 7.54–7.63 (m, 1H), 7.67–7.76 (m, 1H); ^{13}C-NMR (100 MHz, $CDCl_3$, ppm): δ 100.3, 114.9, 117.0, 123.5, 124.4, 133.2, 153.5, 153.7, 160.9; IR; ν_{max} (cm^{-1}) 3052, 2990, 2928, 2852, 2369, 2280, 2219, 2151, 2126, 1812, 1726, 1609, 1561, 1486, 1450, 1386, 1330, 1274, 1253, 1181, 1144, 1021, 938, 853, 761, 714, 641, 508.

Step 4: Synthesis of 4-((1-(2-oxo-2*H*-chromen-4-yl)-1*H*-1,2,3-triazol-5-yl)methoxy)-2*H*-chromen-2-one, L5[37]

To the solution of compound **1** (200.19 mg, 1.0 mmol) and **3** (187.15 mg, 1.0 mmol) in 25 mL of THF:H_2O (2:1), 10 mol% sodium ascorbate (19.81 mg), 3 mol% $CuSO_4{\cdot}5H_2O$ (7.49 mg) and DIPEA (258.5 mg, 2.0 mmol) were added sequentially. The resulting reaction mixture was refluxed for 3 h. After completion of the reaction, the mixture was poured into ice-cold water, the resulting compound was filtered and precipitated with EtOH, followed by recrystallization in ethanol to furnish the pure title compound **L5** as a brown solid with 88% purity (340 mg) yield, M.P. = 229°C; ^{1}H-NMR (400 MHz, $CDCl_3$, ppm): δ 5.59 (s, 2H), 6.24 (s, 1H), 7.04 (s, 1H), 7.35 (t, *J* = 8.0 Hz, 1H), 7.40–7.49 (m, 2H), 7.59 (d, *J* = 8.0 Hz, 1H), 7.67 (dt, *J* = 0.8, 8.8 Hz, 1H), 7.78 (dt, *J* = 0.8, 8.8 Hz, 1H), 7.86 (td, *J* = 0.8, 8.0 Hz, 2H), 9.09 (s, 1H); ^{13}C-NMR (100 MHz, $CDCl_3$, ppm): δ 55.9, 113.7, 116.5, 117.0, 117.9, 123.0, 127.6, 127.7, 127.9, 128.0, 128.9, 129.0, 129.6, 137.3, 137.6, 143.4, 143.5, 143.6, 145.0, 150.1, 151.5; IR; ν_{max} (cm^{-1}) 3134, 3084, 2963, 2922, 2845, 1730, 1618, 1564, 1488, 1447, 1400, 1363, 1326, 1273, 1243, 1184, 1102, 1035, 1002, 936, 834, 752, 643, 528, 499. HRMS (ESI+) m/z for **L5** calcd. $C_{21}H_{13}N_3O_5$ $[M+Na]^+$: 410.0753 found 410.0784.

2.2 | UV–vis and fluorescence spectral measurements

A stock solution of chemosensor **L5** (1×10^{-3} M) was prepared in DMSO, followed by preparation of a sample solution of **L5** (10 μM) in phosphate-buffered solution (20 mM, DMSO:H_2O 1:9, v/v, pH 8.0) in a quartz cuvette (1 cm × 1 cm), and final addition of 10 μl of aqueous stock solution (1×10^{-3} M) of metal salt (K^+, Na^+, Ba^{2+}, Ca^{2+}, Mg^{2+}, Cr^{3+}, Mn^{2+}, Fe^{3+}, Co^{2+}, Ni^{2+}, Cu^{2+}, Zn^{2+}, Pb^{2+}, Ag^+, Al^{3+}, Cd^{2+}, Hg^{2+}, Hg^+ and Sn^{2+}). Fluorescence spectra of the chemosensor **L5** were recorded with a slit width of 3 nm.

3 | RESULTS AND DISCUSSION

3.1 | Colorimetric and fluorimetric responses of L5 to Pb^{2+} ion

The optical properties of chemosensor **L5** (10 μM) were studied using absorption and fluorescence emission spectroscopy at room temperature in 1:9 v/v DMSO:H_2O using phosphate-buffered solution at pH 8.0. The chemosensor **L5** displayed a strong absorption band located at 390 nm which was attributed to the π–π* transition. Upon addition of 20 equiv. of various metal ions of environmental relevance such as Na^+, K^+, Ag^+, Ca^{2+}, Ba^{2+}, Cr^{3+}, Mn^{2+}, Fe^{3+}, Co^{2+}, Ni^{2+}, Zn^{2+}, Cu^{2+}, Pb^{2+}, Cd^{2+}, Hg^{2+}, Sn^{2+}, Al^{3+} and Hg^+ as nitrate salts to the solution of chemosensor **L5**, only Pb^{2+} ion showed high affinity with the development of a new band at 410 nm. The position changes in bands were associated with a perceived color generation from colorless to yellow that could easily be detect by the naked eye in contrast with other metal ions, for which no significance changes were observed (Figures 1a and 2a).

To validate the selectivity of chemosensor **L5**, the absorption titration experiment was also performed. Upon addition of 0–20 equiv. of Pb^{2+} to the solution of chemosensor **L5**, the absorbance at 390 nm

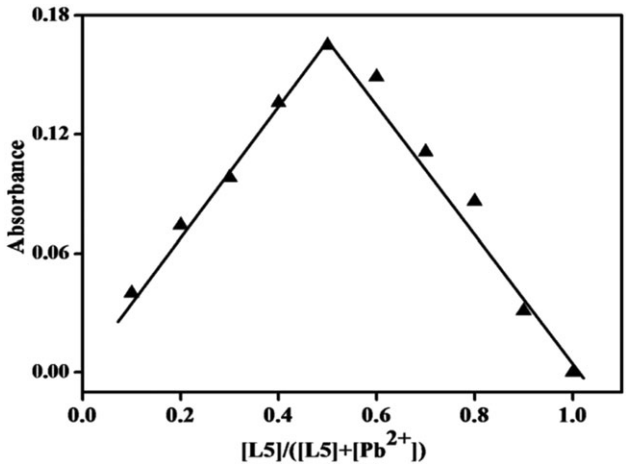

FIGURE 3 Job's plot of the [**L5** + Pb^{2+}] complex in phosphate-buffered solution [20 mM 1:9 DMSO/H_2O (v/v), pH 8.0]

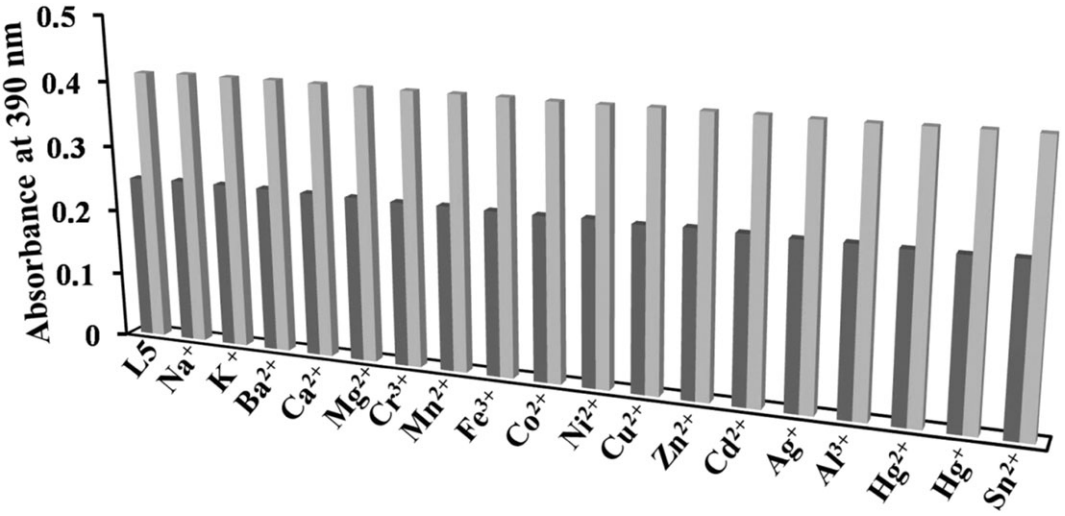

FIGURE 4 Selectivity and competition studies of **L5** (10 μM) with Pb^{2+} in presence of other metal ions in phosphate-buffered solution [20 mM, 1:9 DMSO/H_2O (v/v), pH 8.0]. Grey and black bars represent the absorbance of the [**L5** + metal ions] system and the **L5**+Pb^{2+} system in the presence of 20 equiv. of some metal ion respectively

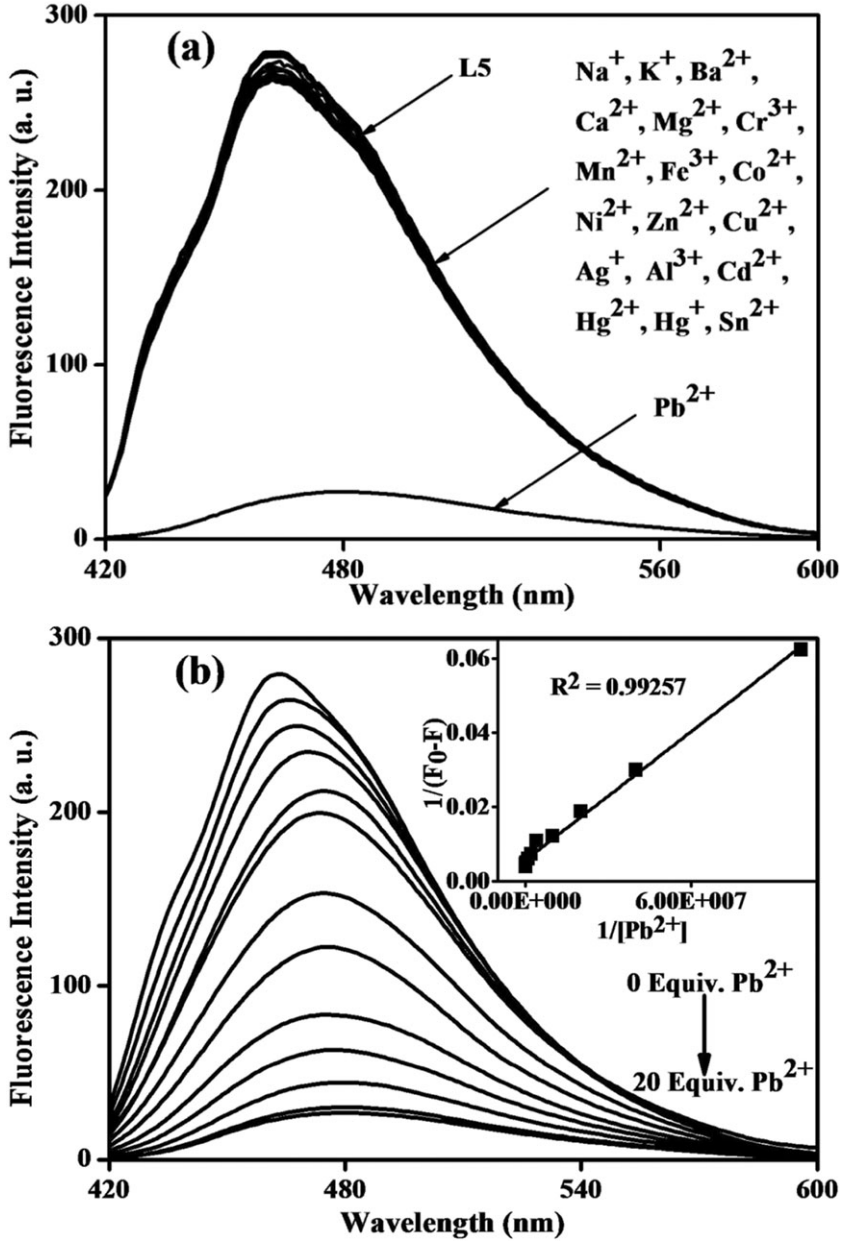

FIGURE 5 (a) Fluorescence responses of chemosensor **L5** (1.0 μM) in phosphate-buffered solution [20 mM, 1:9 DMSO/H_2O (v/v), pH 8.0] to various metal ions (20 μM). (b) Fluorescence responses of chemosensor **L5** (1.0 μM) in phosphate-buffered solution [20 mM, 1:9 DMSO/H_2O (v/v), pH 8.0] to various concentrations of Pb^{2+} (0–20 μM). The inset in (b) shows a Stern–Volmer (SV) plot λ_{ex} = 390 nm, λ_{em} = 462 nm

gradually decreased and, accordingly, one new lower-energy band emerged around 410 nm with a well defined isosbestic point at 417 nm (Figure 2b). Saturation in the absorption spectra was produced by the addition of 20 equiv. of Pb^{2+} relative to **L5**, implying that the efficient cation reception event was consummate. Moreover, level of color change was not influenced by the addition of >20 equiv. of metal Pb^{2+} cations. The appearance of a clear isosbestic points at 417 nm indicated the formation of a strong complexation between the chemosensor **L5** and Pb^{2+}. Job's method observed by absorption spectra was applied to obtain the binding stoichiometry of **L5** with Pb^{2+} in the complex. Absorbance at 390 nm was plotted against a mole fraction of **L5** at a constant total concentration of **L5** and Pb^{2+}, which indicated the 1:1 binding stoichiometry of **L5** with Pb^{2+} in the complex (Figure 3).[38]

The association constant of **L5** with Pb^{2+} was calculated using an SV plot, and was found to be 4.59×10^6 M^{-1} (Figure 2b inset), with a detection limit of 3.16 nM (Figure S7), implying that Pb^{2+} had high affinity for **L5**.[39–41] To explore further the efficacy of **L5** as a Pb^{2+} ion-selective chemosensor, competition experiments were performed in which **L5** was first incubated with various metal cations, and then Pb^{2+} was added. The competition-based absorbance profiles for these metal ions are shown in Figure 4. The distinct responses of selectivity and interference studies revealed that **L5** could be used to distinguish Pb^{2+} ions from many other metal ions.

To demonstrate the ability of chemosensor **L5** to function as a fluorescent sensor for Pb^{2+}, we performed a fluorescence emission experiment in 20 mM 1:9 v/v DMSO:H_2O phosphate-buffered solution at pH 8.0. The chemosensor **L5** display a high emission band at 463 nm with an excitation wavelength of 390 nm and absolute quantum yield (Φ_f = 0.76). Upon interaction with different metal ions (20 equiv.), only Pb^{2+} showed quenching with absolute fluorescence quantum yield (ϕ_f = 0.054) (Figure 5a). To understand the binding ability of chemosensor **L5**, the corresponding emission titration experiment was conducted using Pb^{2+}. By adding Pb^{2+}, the emission intensity at 463 nm corresponding to chemosensor **L5** gradually decreased, and red-shifted to 480 nm when 20 equiv. of Pb^{2+} was added to the system (Figure 5b), which may be attributed to the formation of the receptor–metal complex (Scheme 2) via heavy atom spin-orbit coupling[42], energy or electron transfer.[43] These results suggested that **L5** can act as a 'switched on-off' fluorescence sensor for Pb^{2+} ions particularly. Additionally, the addition of Pb^{2+} made the fluorescence color clearly change from colorless to blue (Figure 1b).

To explain this complex formation further, the binding stoichiometry of the chemosensor **L5**-Pb^{2+} system was determined by way of continuous-variation method (Job plots), wherein the variation of the emission intensity at 462 nm was plotted against the molar fraction of the chemosensor **L5**. The maxima was evidently observed at 0.5 and indicated that the **L5** and Pb^{2+} a formed 1:1 complex (Figure 6a). The binding constant for chemosensor **L5** with Pb^{2+} was evaluated by SV plot, with an association constant 6.76×10^6 M^{-1} (Figure 5b inset) and detection limit of 1.9 nM (Figure S8). The limit of detection for Pb^{2+}, obtained in the present study was compared with the other methods reported in the literature and is given in Table 1. From the Table 1 it is evident that the limit of detection obtained in our method is the lowest for Pb^{2+} ion.

We measured the fluorescence lifetime (τ) of bare chemosensor **L5** to be 7.66 nsec using 390 nm as the excitation wavelength. The lifetime of **L5** was shortened to 6.36 nsec after the addition of Pb^{2+} ions. The change in **L5** lifetime indicates the strong interaction of receptor

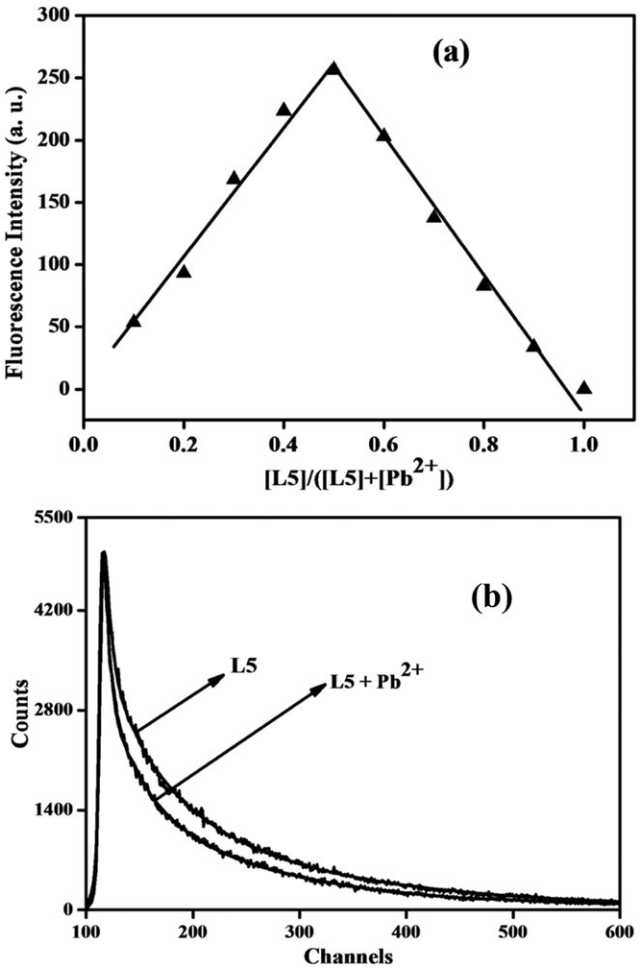

FIGURE 6 (a) Job's plot of the **L5** + Pb^{2+} complex in phosphate-buffered solution [20 mM, 1:9 DMSO/H_2O (v/v), pH 8.0]. (b) Lifetime fluorescence spectra of **L5** in the absence or presence of Pb^{2+} ion with excitation at 390 nm

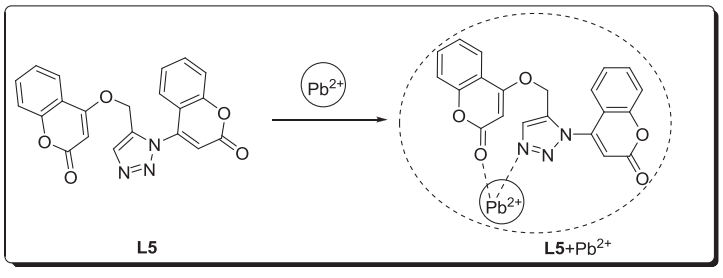

SCHEME 2 Proposed sensing mechanism of compound **L5** for Pb^{2+}

TABLE 1 A comparison of detection limit obtained in the present study with other reported fluorometric methods

Type of probe	LOD	Merits of probe	Mode of assay	Reference
Imidazopyridine-ferrocene dyad	1.32×10^{-8} M	Colorimetric and fluorometric	'Turn-on'	[17]
Triazole-tethered ferrocene–anthracene conjugates	2.0×10^{-9} M	Colorimetric and fluorometric	'Turn-on'	[18]
Triazole substituted 8-hydroxyquinoline (8-HQ)	3.36×10^{-8} M	Colorimetric and fluorometric	'Turn-on'	[26]
1,3,6-trihhdroxy Xanthone	1.8×10^{-7} M	Fluorometric	'Turn-on'	[44]
BSA–Cu NCs	1.0×10^{-8} M	Fluorometric	Quenching	[45]
Azino *bis*-Schiff base	8.0×10^{-9} M	Colorimetric and fluorometric	'Turn-on'	[46]
Coumarin- triazole	1.9×10^{-9} M	Colorimetric and fluorometric	Quenching	This work

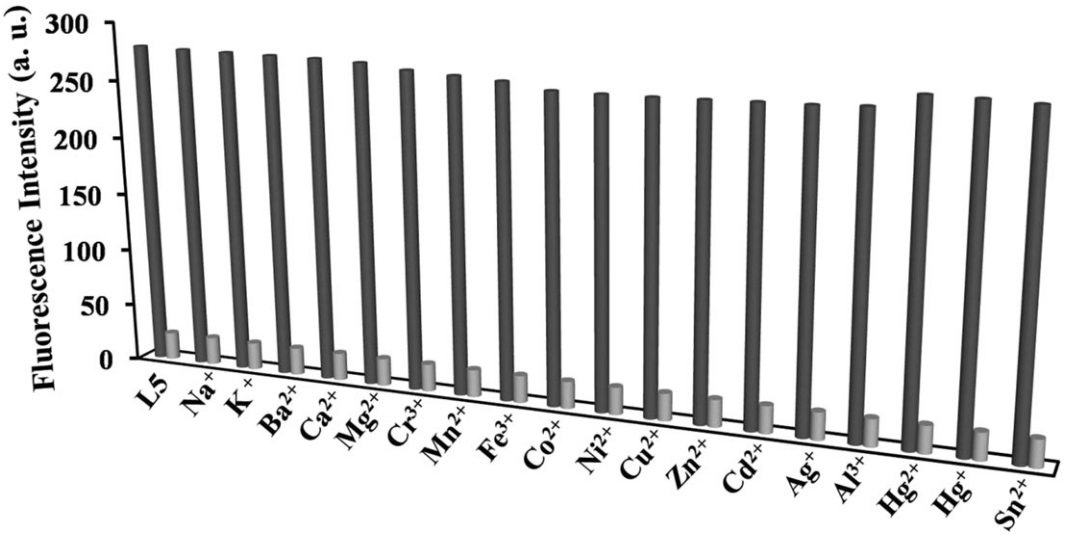

FIGURE 7 Selectivity of **L5** (10 μM) in phosphate-buffered solution [20 mM, 1:9 DMSO/H_2O (v/v), pH 8.0]. Black bars and grey bars represent the fluorescence intensity of [**L5** + metal ions] system and the **L5**+Pb^{2+} system in the presence of 20 equiv. of different metals respectively. λ_{ex} = 390 nm, λ_{em} = 462 nm

L5 with Pb^{2+} ions (Figure 6b). The preferential sensitivity of chemosensor **L5** for selective detection of Pb^{2+} ion was performed by competition experiment in presence of other tested metal ions (20 equiv.). As shown in Figure 7, no interference was observed while performing the competition experiment. Therefore, receptor **L5** was employed as an excellent chemosensor for the detection of Pb^{2+} ions.

3.2 | Nature of binding interactions of L5 with Pb^{2+}

The interaction of chemosensor **L5** and the Pb^{2+} ion was also investigated by FT-IR and HRMS spectroscopy. We measured the FT-IR spectra of chemosensor **L5** and its complex with Pb^{2+} to examine their binding sites (Figure S10). The discrete vibrations located at 3134, 3084 cm^{-1} and ~1730 cm^{-1} in the IR spectrum of **L5** were respectively assigned to the C_{sp2}–H stretching vibration of the benzene ring and the carbonyl group (C=O) stretching vibration of the lactone on the coumarin moiety. When binding with Pb^{2+} ion, a new significant vibration located at 1547 cm^{-1} appeared which was attributed to the N=N stretching vibration of the triazole structure, because N=N was fixed and showed a strong IR signal upon binding with Pb^{2+} ions. The vibration wavelength corresponding to the C=O stretching vibration slightly shifted to 1726 cm^{-1} after binding with Pb^{2+} ions, which indicated that the C=O group of the coumarin moiety attached to an alkoxy oxygen participating in interaction with Pb^{2+}. Therefore, the observed FT-IR data clearly suggested that chemosensor **L5** can chelate Pb^{2+} through interaction with the carbonyl group (C=O) oxygen and triazole nitrogen and form the **L5**+Pb^{2+} complex. Moreover, HRMS (ESI+) data for **L5** calcd. $C_{21}H_{13}N_3O_5$ $[M+Na]^+$: 410.0753 found 410.0784 and for **L5**+Pb^{2+} calcd. $C_{21}H_{13}N_3PbO_5$ $[M+Na+Pb^{2+}]^+$: 618.0508, found 618.0935, suggested that there is a 1:1 complexation between **L5** and Pb^{2+} (ESI, Figures S6 and S9).

To further understand the binding behaviour of **L5** with Pb^{2+}, density functional theory (DFT) calculations were performed for **L5** and **L5**+Pb^{2+} (Figure 8). Structural optimization and computational calculations were carried out using the Gaussian09 quantum chemistry package and results were viewed with GaussView 5. In the present scenario, DFT supported B3LYP/6-31G model chemistry was implemented particularly for **L5**, whereas for metal complexes LANL2DZ (Los Alamos National Laboratory 2-double-z–Acronyms) was used as a basis set to optimize the geometry of the complex. The optimized structure of **L5** and the **L5**+Pb^{2+} complex showed that the Pb^{2+} ion binds to **L5** at nitrogen atoms of the triazole and carbonyl groups of lactone on the coumarin moiety, with Pb–N and Pb–O bond lengths 2.368 Å and 2.032 Å, respectively. Moreover, in the highest energy occupied molecular orbital (HOMO) of **L5**, electron density is mainly located on the coumarin moiety

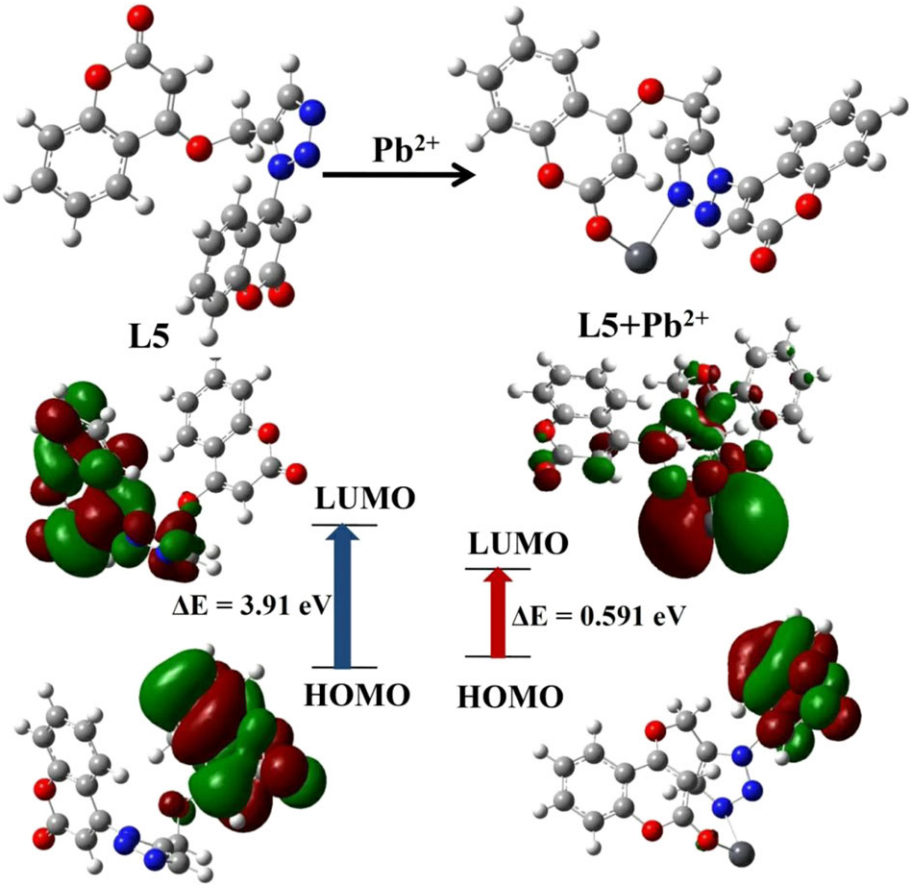

FIGURE 8 Optimized structure, calculated HOMO and LUMO of **L5** and **L5**+Pb^{2+}

which is attached with alkoxy oxygen atom whereas in the lowest unoccupied molecular orbital (LUMO) electron density is located on the coumarin moiety which is attached to triazole ring. However, for **L5**+Pb^{2+}, in the HOMO the electron density is mainly localized on the coumarin moiety which is attached to a triazole ring, while in the LUMO the electron density is localized on the Pb^{2+} ion, indicating a strong ligand-to-metal charge transfer (LMCT) process. The corresponding energy values indicated that the energy gap between the HOMO and LUMO orbitals of the **L5**+Pb^{2+} complex was lower than **L5**, which might be responsible for the bathochromic shift of **L5** upon complexation with Pb^{2+} in the UV–vis absorption spectra.

4 | APPLICATION

4.1 | Visual color changes on TLC plates

To investigate the potential application of **L5** as a metal ion sensor in the solid state, we have prepared a test kit using TLC plates coated with a solution of **L5** (10 μM) followed by drying in air. The color of the TLC plate changed to bright yellow as well as becoming non-fluorescent under irradiation with long UV light only for Pb^{2+} ions, supporting the practical applicability of receptor **L5**. This experiment demonstrates that compound **L5** has the potential to detect Pb^{2+} ions in the solid state (Figure 9).

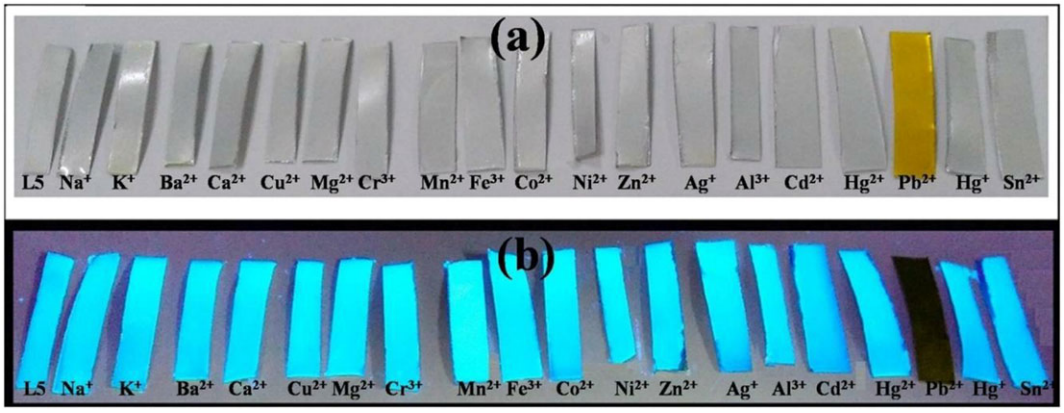

FIGURE 9 Photographs of (a) colorimetric, and (b) fluorometric test kits: thin layer chromatography (TLC) coated with **L5** (1 mM) for detecting Pb^{2+} in phosphate-buffered solution [20 mM, 1: 9 DMSO/H_2O (v/v), pH 8.0]

5 | CONCLUSION

In conclusion, we have successfully developed a coumarin–triazole scaffold as the fluorescent sensor **L5** for Pb^{2+} detection when compared with other competitive metal ions, e.g. K^+, Na^+, Ag^+, Ca^{2+}, Ba^{2+}, Cr^{3+}, Mn^{2+}, Fe^{3+}, Ni^{2+}, Co^{2+}, Zn^{2+}, Cu^{2+}, Pb^{2+}, Cd^{2+}, Hg^{2+}, Sn^{2+} Al^{3+} and Hg^+. The chemosensor works as both as a colorimetric and 'turn-off' fluorescence probe for Pb^{2+}. Significant fluorescence quenching was observed with chemosensor **L5** in the presence of Pb^{2+} ions, while the presence of other metal ions caused no change in fluorescence intensity. This sensor has the capability to detect Pb^{2+} in the nano-molar range with detection limits of 1.9 nM. Changes in the chemosensor can be seen by the naked eye and can be used as an optical sensor for Pb^{2+} determination with significant color changes on TLC plates. This easy, economical, and reliable method has advantages over other reported methods for the detection of Pb^{2+} ions.

ACKNOWLEDGMENTS

We thank the Ministry of Human Resource and Development (MHRD), New Delhi, India (grant number MHR01-23-200-428) for financial support.

ORCID

Shaily http://orcid.org/0000-0003-2196-8558
Ajay Kumar http://orcid.org/0000-0002-6237-7335

REFERENCES

[1] A. R. Flegal, D. R. Smith, *Environ. Res.* **1992**, *58*, 125.
[2] H. N. Kim, W. X. Ren, J. S. Kim, J. Yoon, *Chem. Soc. Rev.* **2012**, *41*, 3210.
[3] H. Needleman, *Annu. Rev. Med.* **2004**, *55*, 209.
[4] Department of Health and Human Services and Prevention, Center for Disease Control, *Morb. Mort. Wkly Rep.* **2003**, *52*, 1.
[5] K. Steenland, P. Boffetta, *Am. J. Ind. Med.* **2000**, *38*, 295.
[6] S. Araki, H. Sato, K. Yokoyama, K. Murata, *Am. J. Ind. Med.* **2000**, *37*, 193.
[7] C. Winder, N. G. Carmichael, P. D. Lewis, *Trends Neurosci.* **1982**, *5*, 207.
[8] D. A. Cory-Slechta, *Adv. Behav. Pharmacol.* **1984**, *4*, 211.
[9] C. M. Bouton, L. P. Frelin, C. E. Forde, H. A. Godwin, J. Pevsner, *J. Neurochem.* **2001**, *76*, 1724.
[10] The European Parliament and the Council of the European Union, Directive on the Restriction of the Use of Certain Hazardous Substances in Electrical and Electronic Equipment **2002**/95/EC.
[11] World Health Organization, *Guidelines for Drinking-Water Quality*, 4th ed., WHO Press, Geneva, Switzerland **2011**.
[12] Y.-Y. Chen, H.-T. Chang, Y.-C. Shiang, Y.-L. Hung, C.-K. Chiang, C.-C. Huang, *Anal. Chem.* **2009**, *81*, 9433.
[13] Agency for Toxic Substances and Disease Registry Case Studies in Environmental Medicine (CSEM) Lead Toxicity, http://www.atsdr.cdc.gov/HEC/CSEM/lead/standards_regulations.html, **2006**.
[14] B. J. Feldman, J. D. Osterloh, B. H. Hata, A. D'Alessandro, *Anal. Chem.* **1994**, *66*, 1983.
[15] R. J. Bowins, R. H. McNutt, *J. Anal. At. Spectrom.* **1994**, *9*, 1233.
[16] M. R. Cave, O. Butler, R. N. Chenery, J. M. Cook, M. S. Cresser, D. L. Miles, *J. Anal. At. Spectrom.* **2001**, *16*, 194.
[17] F. Zapata, A. Caballero, A. Espinosa, A. Tárraga, P. Molina, *J. Org. Chem.* **2009**, *74*, 4787.
[18] A. Thakur, D. Mandal, S. Ghosh, *Anal. Chem.* **2013**, *85*, 1665.
[19] D. Yanga, X. Liua, Y. Zhoua, L. Luoa, J. Zhanga, A. Huanga, Q. Maoa, X. Chenb, L. Tang, *Anal. Methods* **2017**, *9*, 1976.
[20] C.-T. Chen, W.-P. Huang, *J. Am. Chem. Soc.* **2002**, *124*, 6246.
[21] S. Goswami, R. Chakrabarty, *Eur. J. Org. Chem.* **2010**, 3791.
[22] N. Vasimalai, S. A. John, *Spectrochim. Acta, Part A* **2011**, *82*, 153.
[23] N. Nuñez-Dallos, C. Cuadrado, J. Hurtado, E. Nagles, O. García-Beltran, *Int. J. Electrochem. Sci.* **2016**, *11*, 9855.
[24] G. Pagona, S. P. Economopoulos, G. K. Tsikalas, H. E. Katerinopoulos, N. Tagmatarchis, *Chem. – Eur. J.* **2010**, *16*, 11969.
[25] E. Roussakis, S. A. Pergantis, H. E. Katerinopoulos, *Chem. Commun.* **2008**, 6221.
[26] G. Wu, M. Li, J. Zhu, k. W. Chiu Lai, Q. Tong, F. Lu, *RSC Adv.* **2016**, *6*, 100696.
[27] A. P. W. Arachchilage, F. Wang, V. Feyer, O. Plekan, R. G. Acres, K. C. Prince, *J. Phys. Chem. A* **2016**, *120*, 7080.
[28] R. Nazir, A. J. Stasyuk, D. T. Gryko, *J. Org. Chem.* **2016**, *81*, 11104.
[29] M. Tasior, D. Kim, S. Singha, M. Krzeszewski, K. H. Ahn, D. T. Gryko, *J. Mater. Chem. C* **2015**, *3*, 1421.
[30] Shaily, A. Kumar, N. Ahmed, *Supramol. Chem.* **2017**, *29*, 146.
[31] Shaily, A. Kumar, S. Kumar, N. Ahmed, *RSC Adv.* **2016**, *6*, 108105.
[32] Shaily, A. Kumar, N. Ahmed, *Ind. Eng. Chem. Res.* **2017**, *56*, 6358.
[33] Shaily, A. Kumar, N. Ahmed, *New J. Chem.* **2017**, *41*, 14746.
[34] C. P. Rao, G. Srimannarayana, *Synth. Commun.* **1990**, *20*, 535.
[35] K. C. Majumdar, S. K. Samanta, *Tetrahedron Lett.* **2002**, *43*, 2119.
[36] T. Saito, T. Ohkubo, H. Kuboki, M. Maeda, K. Tsuda, T. K. S. Satsumabayashi, *J. Chem. Soc., Perkin Trans.* **1998**, *1*, 3065.
[37] F. Himo, T. Lovell, R. Hilgraf, V. V. Rostovtsev, L. Noodleman, K. B. Sharpless, V. V. Fokin, *J. Am. Chem. Soc.* **2005**, *127*, 210.
[38] A. Senthilvelan, I. T. Ho, K. C. Chang, G. H. Lee, Y. H. Liu, W. S. Chung, *Chem. – Eur. J.* **2009**, *15*, 6152.
[39] S. Bano, A. Mohd, A. A. P. Khan, K. S. Siddiqi, *J. Chem. Eng. Data* **2010**, *55*, 5759.
[40] M. Shortreed, R. Kopelman, M. Kuhn, B. Hoyland, *Anal. Chem.* **1996**, *68*, 1414.
[41] W. Lin, L. Yuan, Z. Cao, Y. Feng, L. Long, *Chem. – Eur. J.* **2009**, *15*, 5096.
[42] D. S. McClure, *J. Chem. Phys.* **1952**, *20*, 682.
[43] A. W. Varnes, R. B. Dodson, E. L. Wehry, *J. Am. Chem. Soc.* **1972**, *94*, 946.
[44] D. Karak, A. Banerjee, S. Lohar, A. Sahana, a. S. K. Mukhopadhyay, S. S. Adhikari, D. Das, *Anal. Methods* **2013**, *5*, 169.
[45] D. Feng, W. Zhu, G. Liu, W. Wang, *RSC Adv.* **2016**, *6*, 96729.
[46] A. Ghorai, J. Mondal, R. Saha, S. K. Bhattacharya, G. K. Patra, *Anal. Methods* **2016**, *8*, 2032.

SUPPORTING INFORMATION

Additional Supporting Information may be found online in the supporting information tab for this article.

How to cite this article: Shaily, Kumar A, Parveen I, Ahmed N. Highly selective and sensitive coumarin–triazole-based fluorometric 'turn-off' sensor for detection of Pb^{2+} ions. *Luminescence*. 2018;1-9. https://doi.org/10.1002/bio.3468